FIRST PRINCIPLE INVESTIGATIONS ON THE ELECTRONIC STRUCTURES OF GRAPHENE NANORIBBON AND ITS INTERACTIONS WITH MUONIUM

ANG LEE SIN

UNIVERSITI SAINS MALAYSIA

2010

FIRST PRINCIPLE INVESTIGATIONS ON THE ELECTRONIC STRUCTURES OF GRAPHENE NANORIBBON AND ITS INTERACTIONS WITH MUONIUM

by

ANG LEE SIN

Thesis submitted in fulfillment of the requirements for the

Degree of Doctor of Philosophy

NOVEMBER 2010

ACKNOWLEDGMENT

I would like to express my deepest gratitude first and foremost to my supervisors Associate Professor Dr Shukri Sulaiman and Associate Professor Dr Mohamed Ismail Mohamed Ibrahim for providing me the most appreciated guidance, advice, and support in order to complete my study.

To all my friends who have ever helped me directly and indirectly in this project. Thank you for the companionship and the encouragement.

Last but not least, I would like to dedicate this thesis to my parents and family for their everlasting moral support and faith towards me. Thank you very much.

TABLE OF CONTENTS

LIST OF TABLES

LIST OF FIGURES

LIST OF ABBREVIATIONS

AFM: Antiferromagnetism

AGQD: Armchair-edged graphene quantum dot

AM1: Austin Model 1

AO: Atomic orbital

au: atomic unit

B3LYP: Becke 3-parameter exchange hybrid functional with Lee Yang Parr correlation functional

CNG: Carbon nanographene

CC: Coupled cluster

CI: Configurational interaction

CVD: Chemical vapour deposition

DFT: Density functional theory

ESR: Electron spin resonance

G03: Gaussian 03

GNR-Mu: Graphene nanoribbons-Muonium

HF: Hartree-Fock

HOMO: Highest Occupied Molecular Orbital

FM: Ferromagnetism

GNR: Graphene Nanoribbon

GQD: Graphene quantum dot

GTO: Gaussian-type orbitals

GVB: Generalised valence bond

LCAO: Linear combination of atomic orbitals

LUMO: Lowest Unoccupied Molecular Orbital

MBPT: Many-body perturbation theory

MCSCF: Multiconfigurational self consistent field

Mu: Muonium

MO: Molecular Orbital

MP2: Møller-Plesset second order correction

MP3: Møller-Plesset calculation third order correction

MP4: Møller-Plesset fourth order correction

OS: Open-shell singlet

PBE: Exchange/correlation functional of Perdew, Burke, and Ernzerhof

PBEPBE: Exchange and correlation functionals of Perdew, Burke, and Ernzerhof

PBE0/PBE1PBE: Hybrid functionals of Perdew, Burke, and Ernzerhof

PAH: Polyaromatic hydrocarbons

ROHF: Restricted open Hartree-Fock

SCF: Self consistent field

SOMO: Singly occupied molecular orbital

STO: Slater-type orbitals

LIST OF SYMBOLS

H: Hamiltonian

E: Energy

ε_k: Eigenvalue/Energy *k*

e: charge of electron

Φ : Wavefunction

Ψ^{HP} : Hartree product

r_i : position of electron *i*

$\vec{R}_i$: position of nucleus *i*

$\{\vec{r}_i, m_{si}\}$: position and spin coordinates of electron *i*

$\psi_i(\vec{r})$: spatial orbital electron *i*

r_{ij}: distance between electron *i* and *j*

Z_α : charge of nucleus α

$\alpha(m_s)$: spin up with spin coordinates m_s

$\beta(m_s)$: spin down with spin coordinates m_s

ρ_j: charge density of electron j

Ψ^{SD}: Slater determinant

δ_{ij}: Kronecker delta function

∇^2: Laplacian operator

$\hbar$: Planck's constant/2π

J_{ij}: Coulomb integral between an electron in ψ_i and another in ψ_j.

K_{ij}: exchange integral between an electron in ψ_i and another in ψ_j.

S_{ij}: overlap integral between an electron in ψ_i and another in ψ_j.

χ_μ: basis functions

$c_{\mu i}$ / $d_{\mu p}$: coefficients

$P_{\mu\nu}$: density matrix

$(\mu\nu|\lambda\sigma)$ or $(ij|ab)$: two-electron integral

$\langle T \rangle$: mean kinetic energy

$\langle V \rangle$: mean potential energy

$d\tau_1$: volume element of electron 1

I_{ij} : Lagrangian multiplier

$F_{\mu\nu}^{\alpha}$: Fock matrix element of alpha electrons

g_p : primitive Gaussians

A_{iso}: isotropic hyperfine constant

A_{dip}: anisotropic hyperfine constant

Q_A : total charge on atom A

KAJIAN PRINSIP PERTAMA KE ATAS STRUKTUR ELEKTRONIK REBEN-NANO GRAFIN DAN SALINGTINDAKAN DENGAN MUONIUM

ABSTRAK

Keputusan yang dilaporkan di sini adalah hasil penyiasatan teoretis ke atas sistem grafin. Dalam pemilihan kaedah penyiasatan, beberapa kaedah pengiraan seperti kaedah orbit molekul, pasca medan konsisten-kendiri, dan teori fungsi ketumpatan (dalam bentuk fungsi tulen dan hibrid) telah dipertimbangkan. Kaedah B3LYP merupakan kaedah yang paling sesuai untuk penyiasatan ini kerana kaedah-kaedah yang lain mempunyai masalah pencemaran spin dan masalah kecekapan. Untuk menentukan model yang sesuai bagi kegunaan pengiraan klaster orbit molekul, dua set model reben-nano grafin telah dikaji, satu model dengan tepian zigzag dan satu lagi dengan tepian lengan-kerusi. Sifat-sifat elektronik dan geometri reben-nano grafin telah didapati mempunyai kebergantungan terhadap saiz reben-nano grafin tersebut. Analisis orbit molekul, ketumpatan spin, cas, dan jarak ikatan bagi model-model tersebut menunjukkan bahawa untuk saiz tertentu, ciri-ciri elektronik bagi model yang digunakan ini menghampiri ciri-ciri elektronik reben-nano grafin dengan panjang infinit.

Untuk penjerapan muonium pada satah dasar reben-nano grafin, tapak yang paling stabil adalah kedudukan di mana muonium bersambung terus kepada atom karbon. Analisis interaksi antara muonium dan reben-nano grafin menunjukkan bahawa LUMO dan HOMO sistem adalah kebanyakannya sumbangan dari reben-nano grafin. Pada tapak yang paling stabil, ungkapan sentuhan Fermi untuk reben-nano grafin bertepi lengan-kerusi ialah 111 MHz dan 129 MHz untuk reben-nano grafin bertepi zigzag.

Gandingan-gandingan anisotropik adalah kecil. Penemuan-penemuan hasil penyiasatan ini boleh dijadikan sebagai rujukan untuk menjalankan eksperimen yang menggunakan muonium untuk mengenalpasti jenis tepian untuk sesuatu reben-nano grafin.

FIRST PRINCIPLE INVESTIGATIONS ON THE ELECTRONIC STRUCTURE OF GRAPHENE NANORIBBON AND ITS INTERACTION WITH MUONIUM

ABSTRACT

The results reported here are from the theoretical investigations of the graphene systems. In selecting the suitable methods for use in the simulations, a few methods, ranging from molecular orbital, post-self-consistent field, and density functional theory (in the forms of pure and hybrid functionals) are selected. B3LYP emerged as the suitable choice for use in the investigations as other methods suffer from spin contamination and the problem of efficiency. In order to find the models that are suitable for use in molecular orbitals cluster calculations, two sets of graphene nanoribbon models, one with zigzag and the other the armchair edges were investigated. It was found that the electronic properties and the geometries of the graphene nanoribbons do depend on the size of the graphene nanoribbons. Analysis of molecular orbitals, spin densities, charges and bond lengths of the models show that for a certain size, the electronic properties of the models mimic those of the infinitely long graphene nanoribbons. For the adsorption of muonium on the basal plane of a graphene nanoribbon, the site where the muonium connects directly to the carbon atom is the most stable site. From the analysis of the interactions between muonium and the underlying graphene nanoribbons, LUMO and HOMO of the systems are mostly from the graphene nanoribbons. At the most stable site, the Fermi contact term is 111 MHz for armchair-edged GNR and 129 MHz for zigzag-edged GNR, while the anisotropic couplings are negligible. These findings can be the reference in performing experiment that use muon to identify the type of the edges of a graphene nanoribbons.

CHAPTER 1

INTRODUCTION TO GRAPHENE

1.1 Introduction

The discovery of graphene, a two dimensional sheet of carbon atoms, has generated great interest in the scientific community. It was first obtained by mechanical exfoliation and originally categorized into a class of materials that should not exist because of thermal instability [1,2]. Since the successful separation of graphene sheets from the bulk graphite, research activities have been thriving in this area because of possible revelations of new knowledge in condensed matter physics and their potential applications. One of the possible applications of graphene is in nanoelectronics [3]. A few reviews on the electronic and structural properties of graphene have been published [3-7]. The Nobel Prize in Physics of 2010 was awarded to Andre Geim and Konstantin Novoselov for their experiments that led to the discovery of graphene.

Before the discovery of free standing graphene, the electronic structure of graphene layer has been the subject of a few theoretical calculations. The reason is that the large 3.35 Å layer-to-layer separation between adjacent layers of graphite minimizes the interaction between two adjacent layers, thus graphene layer can be taken as the first approximation of graphite. In 1947, Wallace calculated the band structure of two dimensional (2D) graphite using the tight-binding method, and found that 2D graphite is a semiconductor with zero activation energy [8]. This is followed by the theoretical works of Mrozowski [9], McClure [10], Slonczewski and

Weiss [11], and Painter and Ellis [12]. These are the pioneer works of theoretical calculations on two- and three-dimensional graphite.

Graphene is a zero energy gap semiconductor but when it is fully hydrogenated at both the basal planes, it becomes a semiconductor [13]. This predicted material, known as graphane [13], has been synthesized experimentally [14]. In another case, where the graphene sheet becomes semihydrogenated, that is, only one side of the basal plane is fully hydrogenated, the energy gap (0.46 eV) becomes smaller than that of graphane [15]. This material, coined as graphone, was demonstrated to be stable at room temperature and show ferromagnetism in the ground state [15,16].

Despite the impressive electronic properties and the high crystal quality, graphene does have its shortcomings. The lack of an energy gap in graphene layers is a hindrance to its potential usage as electronic materials. A few methods have been proposed to create an energy gap in the graphene structures. One method is by epitaxially growing graphene on a bulk substrate [17]. The gap obtained in this way is attributed to the symmetry breaking of the A-B sublattices when placed on a substrate. Using graphene in the form of nanoribbons is another way of obtaining energy gaps [18].

Since the investigations reported in this work utilised the cluster method, the edges on graphene are a big concern. Typically, there are two types of edges on graphene. One is designated zigzag, and the other is armchair. They are shown in Figure 1.1 (a). The electronic properties of these two edges are different, especially on graphene nanoribbons (GNRs). Recently, there have been suggestions of a third type of edge on graphene [19-24]. The new edge, as shown in Figure 1.1 (b) is

designated as reczag and is formed by the rearrangement of the hexagons in the zigzag edges into alternating pentagons and heptagons [23]. This edge is said to be more stable than the zigzag or armchair edges [23].

In the following parts of this chapter, the literature review on the experimental and theoretical studies on the electronics and structural properties of graphene systems that have been reported in the literatures will be presented. Also presented will be the fabrications and potential uses of graphene and graphene nanoribbons.

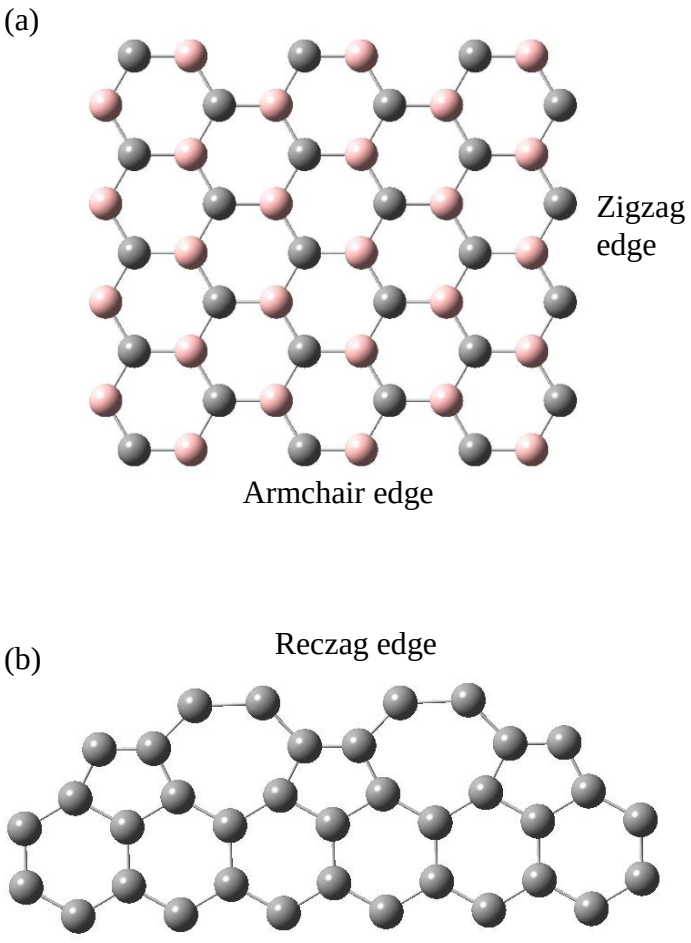

Figure 1.1. (a) Fragment of a graphene showing the zigzag and armchair edges. The colours show the lattices of A and B. (b) Reczag edge that was proposed to be more stable than armchair and zigzag edge. The bond lengths and angle are taken from Ref. [19].

1.2 Geometrical Properties of Graphene

A graphene sheet can be viewed as a single layer of hexagonally arranged carbon atoms pulled out from the bulk graphite. It can be viewed as two lattices A and B arranged in alternating fashion, as shown in Figure 1.1(a) by two different colour schemes. A graphene sheet is not a perfectly flat structure. There is experimental evidence of ripples in suspended graphene sheets [25], and computer simulations suggest that the bonding between carbon atoms in graphene may be the cause for the ripples [26]. Based on the observation from images of transmission electron microscopy, it was proposed that graphene layers are not necessarily always rigid, flat and coplanar entities due to the dynamics of the bond lengths [27]. When a force is applied to the graphene sheet, the sheet will endure elastic and reversible deformation before it fractures [28,29]. There is no experimental observations of the C−C bond length in a graphene sheet. The value of 1.421 Å is the value of C−C in graphite [30].

It is interesting to know when the C−C bond lengths in the graphene models used in simulations will have the C−C bond lengths in graphite. There have been a few studies performed to find the bond lengths of graphene models. A mathematical equation that predicts the bond lengths for certain edge bonds in hexagonal benzenoid hydrocarbons has been formulated by Morikawa et al. [31]. The prediction of the bond lengths of some small nanoflakes using this equation, which required the calculation of the Pauling bond order, ranges from 1.378 Å to 1.456 Å [31] . The results were verified by AM1 semiempirical calculations [31]. In other studies, using semiempirical methods and larger nanoflakes with D_{2h} symmetry and different arrangements of the edges, it was shown that the bond length at the periphery of the nanoflakes deviated (contracted) the most from the ideal value of 1.421 Å [32-34].

This result, that the edge deviates considerably from the ideal C−C bond, has also been obtained in the study of large graphene molecules with different symmetries, in a series of papers by Philpott et al. [35-39].

Using the B3LYP/6-31G(d) level of theory, Moran et al. found that the internal C−C bond of geometry optimized for polybenzenoid hydrocarbons, with sizes equal to or larger than $C_{48}H_{24}$, will converged to about 1.43 Å [40]. In another paper, using a graphene fragment of $C_{62}H_{20}$, the lengths of the central C−C bonds are 1.410 Å [41]. Using the AM1 theory, Dietz et al. found that the central C−C bond length is 1.42 Å for a 78-carbon hydrocarbon molecule [32]. A larger cluster with 192 carbon atoms was reported by Tyutyulkov et al where the geometry was optimized using a semi-empirical method [33]. It was shown that the central C−C bond has a value of 1.41 Å [33]. Using the same semi-empirical method, the central C−C bond of a 216-carbon cluster with D_{2h} symmetry were calculated to have a length of 1.43 Å [34]. Using Monte Carlo simulations to study the ripples of a graphene sheet, it was noted that the bond lengths ranged from 1.379 Å to 1.437 Å [26]. Large graphene molecules with zigzag and armchair (crenellated) edge have also been the subject of detailed studies [35-39]. The molecules in these studies have a symmetry of D_{3h} (triangular) [35,36] and D_{6h} (hexagon-shaped) [36-39]. For these large graphene molecules, there is a central zone that has all the bonds and angles found in the graphite plane (C−C is 1.42 Å, planar sheet) [35-39]. This result agrees with the one obtained by Stein and Brown in their study of large condensed polyaromatic hydrocarbons using the Huckel molecular orbital theory [42].

Apart from the edges of graphene flakes, the edges of an infinite nanoribbon has also been studied. Tyutyulkov et al. [43] used semi-empirical methods to calculate the geometries for zigzag-edged GNRs and armchair-edged GNRs. For

zigzag-edged GNR, the bond length at the edges ranged from 1.374 Å to 1.412 Å, while the central bonds have length of 1.415 Å. For armchair-edged GNR, the edges have bond lengths of 1.347 Å and 1.393 Å. No clear internal bonds were defined because of the width of the armchair GNR used in this case. On the other hand, calculations utilising periodic boundary conditions showed that for zigzag-edged GNR, the bonds at the edges ranges from 1.404 Å – 1.407 Å, and the bonds at the inner edges ranged from 1.439 Å – 1.458 Å. All other bonds are close to 1.421 Å [44]. Thus from the values given, double bond is non-exist in infinite zigzag-edged GNR [44].

To summarise, the C−C bond lengths at the edges deviate considerably from the value of 1.42 Å in graphite, regardless of the type of graphene. While no definitive conclusions can be made to the pattern of the bond lengths at the center of a GNR, the bond lengths at the center of small graphene nanoflakes depends on the symmetry, size, and type of edge of the finite-sized clusters, and will converge to 1.42 Å, independent of the methods used. Only when large graphene molecules are used will a center region that resemble the graphite plane exists in the graphene models.

1.3 Electronic Properties of Graphene and Graphene Nanoribbons

Graphene has marveled scientists due to its peculiar electronic properties that promise great potential in the electronics industry [3]. When free standing graphene was found [1,2], subsequent experiments confirmed that the electrons that carry the charges behave as relativistic quasiparticles called Dirac fermions [45,46]. This charge carriers can travel submicrometer distances without being scattered and can travel as fast as 15000 $cm^2 V^{-1} s^{-1}$ [1,2,45,46]. This high mobility is due to the

structural purity and high resistance to changes in temperature or the presence of excess charge on the graphene sheet [47]. Recently, a much higher carrier mobility in excess of 10^7 $cm^2 V^{-1} s^{-1}$ was obtained from graphene layers decoupled from bulk graphite [48]. Other interesting properties of graphene are the quantum Hall effect at room temperature [46,49] and the nonzero minimum conductivity [45].

As mentioned in the Introduction section, zigzag and armchair edges have different electronic properties. Mono-hydrogenated zigzag edges in graphene have a localized state known as the edge state [50,51]. It is due to the unsaturated π electrons at the edge and they exist as a flat-band at the Fermi level in the band structure [50,51]. The existence of the edge state has been confirmed by first-principle calculations [52]. The edge state is shown as a bright spots in scanning tunneling microscopy (STM) [53-55]. The existence of these edge states depends on the sequence of zigzag sites at the zigzag edge [51], and they decay exponentially towards the centre of GNR [50,51]. With the application of a magnetic field, modifications can be made to the edge states [56]. Conductivity at these edges is higher than those that do not have this edge state [57] and it is valid for both H-terminated and non H-terminated edges [58]. This result is in line with those from energy considerations, where the armchair edge, which has no edge state, has energy which is lower by 0.2 eV/Å per edge atom as compared to the zigzag edge [59]. Thus, armchair edge is more stable than zigzag edge. Huang et. al. use the edge stress and edge energy in the study of the stability of graphene edges and found that for the case of the zigzag edge, these edge stress and edge energy depends only weakly on the width of the GNR [22].

Theoretical and experimental studies show that the band gap of GNR varies inversely with the width [18,60,61]. Disagreements occurred in predicting the

metallicity of the zigzag-edged GNR and armchair-edged GNR. Tight-binding calculations have shown that zigzag-edged GNRs are always metallic [50-52,62-67], while first-principle calculations have shown that zigzag-edged GNRs are only metallic when both the edges have ferromagnetic (FM) configurations or no spin polarization at the edges [68]. Gap opening in the zigzag GNR is available only in the antiferromagnetic state [68]. Also, using tight binding calculations, armchair-edged graphene nanoribbons were predicted to be metallic or semiconducting [50,51,65-67]. Only when the GNR width is $3M-1$, where M is an integer, will the GNR is metallic [51]. However, results from first principles calculations showed that armchair-edged GNR always has a band gap, and the metallic state is unstable [69]. The causes for the existence of a band gap was given by Son et al. [18]. For armchair-edged GNR, it is due to the quantum confinement at the edges, while for zigzag-edged GNR, it is the magnetic state at the edges. The edge states at the zigzag edge can also show a phenomenon known as half-metallicity when an external electric field is applied [63,70-74].

The band gap of graphene nanoflakes are also subjected to investigations due to its potential applications in electronics. Using the tight-binding method to investigate the electronic properties of zigzag- and armchair-edged graphene quantum dots (GQDs), Zhang and Chang [67] reported that as the size of the GQD increases, the energy gap decreases. This result is similar to that of GNR. The decrease is faster in zigzag edge than in the armchair edge GQD (AGQD). The gap is zero when AGQD goes to infinity.

The ground state of a zigzag-edged nanoribbon is the antiferromagnetic (AFM) configuration, based on predictions using quantum mechanics calculations [18,63] or a method known as the resonance-theoretic method [75]. The resonance-

theoretic method [76,77] bypasses all the tedious quantum mechanical calculations in predicting the spin densities of graphene. The stability trend of the zigzag edges in infinite GNR and polyaromatic hydrocarbons (PAHs) is the same and has the following trend: AFM < FM < nonmagnetic [62,63,72,78]. In the AFM configuration, the spin densities are oppositely oriented at the two edges of the ribbon. The difference in energy between the AFM and FM state is 0.011 eV/edge atom [79]. The zigzag edge atom in the AFM configuration is calculated to have a Mulliken spin density of 0.33 [75]. This value is smaller than 0.471, calculated using first principle methods by Kudin [44]. Recently, Lin et al. showed that the ground state of armchair-edged GNRs does exhibit ferromagnetism [80]. Magnetism of the nanographene structure, which is due to the edge states at the zigzag edges, is resistant to edge defects and edge irregularities [81].

A zigzag-edged GNR can be described by using the number of zigzag lines in a ribbon, denoted as *n*-zigzag-edged GNR. When *n* equals to 1, this corresponds to *trans*-polyacetylene [82] and is the basis of the zigzag-edged GNR. The change in the properties when the zigzag-edged GNR was constructed by adding successive *trans*-polyacetylene to the previous one was investigated by Jiang et al. [82] They investigated the ground state properties of *n*-zigzag-edged GNR, with $n = 1, 2, 3, 4$, and found that the ground state of the ribbons exhibit the AFM configuration for $n = 2$ and above. Hod et al. showed that the minimum conditions for a graphene nanodot to show antifferomagnetism at the zigzag edges is the presence of three consecutive zigzag edges, and the width of the dot must be 1 nm or wider [74].

Banerjee and Bhattacharyya reported, within the of B3LYP/6-31G(d,p) level of theory, that in nano-graphene, the molecular orbitals at the zigzag edges are more conspicuous than those at the armchair edges [83]. In the same paper, using Mulliken

population analysis, it was also reported that the partial charges on the zigzag edge carbon atoms ranged from −0.30 to 0.19, and for armchair edges, the charges ranged from −0.17 to 0.08. Charge distribution for graphene models has also been reported by Ruuska and Pakkenen [84]: by performing the Mulliken population analysis on the wavefunction obtained at HF/6-31G(d) level, the charge at the central carbon atom was shown to be nearly neutral. For large graphene molecules, with a width of a few nanometers, the charges and spin densities attenuated monotonically from the edge to the center [35,36]. The same trend is also observed for spin densities in zigzag-edged GNRs [44].

So far, no study of charge distribution of GNR has been reported. Also, there has been no emphasise on GNR with armchair edges. This may be due to the fact that the edge state is absent from edges of this type, thus the lack of magnetism for armchair-edged GNR. But with appropriate doping, armchair-edged GNR are shown to exhibit ferromagnetism [80]. The dopings to armchair-edged GNR are to tune the charge carriers to a certain concentration. With this finding, both zigzag-edged GNR and armchair GNR shows magnetism, albeit with different scenario.

1.4 Identification of Graphene

In an early paper by Novoselov et al. [2], it was pointed out that the isolation of graphene sheet is not an easy task, as it is time consuming and difficult to locate the single layer of graphene from the substrate. As of today, a few standard microscopy methods are used, together with other approaches which are mentioned below. The findings that zigzag-edged GNR shows edge states and a potential candidate for electronic devices also necessitates methods that can identify graphene.

Identification of the edges of graphene nanoribbons, either as zigzag-edged GNR or armchair-edged GNR have been performed by employing the scanning tunneling microscopy or atomic force microscopy [53-55,85-89], or a combination of both [90]. A video on how the edges are formed is also available [21]. It was also proposed that the specific edges can be determined by the spectra of the bright exciton state of the optical absorption [91] or using Raman peaks [44]. Also, refractive index was suggested as a means to identify the graphene flakes on a three-layer system "graphene-thin film-silicon" by passing a light beam through the system [92]. Another way to identify graphene is to use total colour difference method [93]. This method offers a rapid and accurate way to identify graphenes without destroying it [93].

In this work, a method is suggested to identify the edges of a GNR by exploiting the hyperfine interactions between the nucleus of a muonium and the conduction electrons from graphene. The approach is different from the hyperfine interactions between the nucleus of isotope ^{13}C and the conduction electrons, as have been performed by Yazyev [94] and Fisher et al. [95] in their studies of spin decoherence time in graphene systems. In Yazyev's work, first-principle methods and a few small graphene flakes were used [94]. Apart from the non-zero isotropic hyperfine coupling constants, Yazyev found that the spin of the conduction electrons and the local atomic structure affects the hyperfine interactions in graphene. Furthermore, the hyperfine constant is weaker and more anisotropic than those heavier elements in the solid state environment [94]. Using a bigger graphene model in the shape of a quantum dot, Fisher et al. [95] reported that the isotropic hyperfine constant is zero when the graphene size is extended to its limit, and the contributions of the hyperfine constants arise from the anisotropic hyperfine interactions. Thus the

results of these reports do not agree with each other. The results show that the main contribution of the hyperfine interactions between the muonium and conduction electron at the center region is the Fermi contact term, while the anisotropic terms are negligible. Furthermore, the hyperfine coupling strengths in zigzag-edged GNR and armchair-edged GNR are different. The detail analyses are given in Chapter 5.

1.5 Adsorption on Graphene and Graphene Nanoribbons

Before the discovery of the graphene sheet, theoretical calculations involving graphene layers interacting with other species were performed to get a clearer picture of the reactions, for instance, oxidation and gasification. To model adsorption on graphene using first principles calculations, many sizes and configurations of graphene has been used [96-104].

In theoretical studies, adding hydrogen atoms to the edges of graphene systems is done for two purposes. One is to passivate the dangling bonds, and the other is to obtain a uniform sp^2 hybridization across the graphene sheet. This type of edge with monohydrogenation is known as Fujita's edge [50]. Another method of hydrogenation is to put a methylene group at the zigzag edge and create Klein's edge [105] (or beard edge [106]) and the edge carbon will have sp^3 type of hybridization. These two types of terminations are shown in Figure 1.2. Both Fujita's and Klein's edges will also have edge states. Apart from the hybridizations at the edge carbon atoms, the difference between mono- and di-hydrogenation lies in the existence of π orbital edge states at different regions of the wavevectors, [62] and there are no bonds that has double bond character in monohydrogenated GNR [44]. For the adsorption on the basal plane, the established view is that the hydrogen atoms prefer the direct-bonding site to the carbon atom. A few calculations agreed with this view

[104,107]. Yazyev and Helm considered the hydrogen adsorption in their study of magnetism due to defects in graphene [108]. A single hydrogen atom that was directly attached to carbon atom at the basal plane displaced upward the carbon atom [108]. The neighbouring carbon atoms of this carbon atom were also uplifted slightly [108].

Apart from hydrogen, adsorptions using other atoms have also been studied. When fluorine atoms were adsorbed on the basal plane of a graphene sheet, covalent bonds will be formed between the fluorine and carbon atoms [109]. The π-state at the adsorbed carbon site will be destroyed, thus there are no π-state at the fluorinated site [109]. Adsorption at a Klein's edge using fluorine atoms at the zigzag edges also has resulted in sp^3 hybridizations [44]. But for fluorine atoms, only Fujita's edge show magnetism [110]. Also, the ground state of Klein's edged GNR showed antiferromagnetism at a larger ribbon width compared to those that have Fujita's edge [44]. For metal adatoms on the basal plane of graphene, elements from group 1-3 will bond ionically to the carbon atom, while transition metals with d valence electrons will have covalent bonding [111]. It was pointed out that among these elements, Pd shows magnetism [112]. For lithium, it's a donor with respect to graphite, as it donates electrons to graphite [113]. It was argued that cation-π interaction was responsible for the Li-graphite bonding [113], instead of the existence of gaps of frontier orbitals in the substrate model [100].

When molecules are adsorbed on graphene sheet, the type of interactions between the molecules and graphene sheet depends on the type of molecules. For example, nucleobases have no chemical bonding to the graphene plane, only weak attractions [114,115]. This is attributed to the molecular polarizability that induced attractive forces between the molecules and the graphene sheet [114,115]. Another

view is that the ‘bonding’ is due to the electron exchange and correlation effects [115]. N_2 [97] and O_2 [116] molecules are also adsorbed weakly on the basal plane. It was argued that this is caused by the arrangement of carbon atoms at the site of adsorption [97].

Since the edges of GNR is a candidate for building block for future electronic devices, the edges are subjected to various substitutions in order to alter the electronic properties to suit one’s needs. It was shown that NH_2 termination at both edges of the zigzag-edged GNR can change the conductivity from semiconducting to metallic [117], while terminating zigzag-edged GNRs with ketone or ether will also make the ribbon metallic [68]. But it was reported by Hod et al. that edge oxidation with ether group is unstable with respect to hydrogen edge [70]. The phenomenon of half-metallicity can be induced at a lower electric field when the zigzag-edged GNR is edge-oxidized with hydroxyl and lactone [70].

From the results involving adsorption at the basal plane, it can be seen that species with single atoms are more easily adsorbed to the basal plane of graphene sheet compared to molecules. Although terminating graphenes’ edges with species other than hydrogen can be used to modify the electronic properties of GNRs, it may be technologically challenging to oxidize the edge of the GNR evenly with the same species of atoms. The robustness of the predicted properties also needed to be studied using more realistic GNRs, which includes defects and impurities.

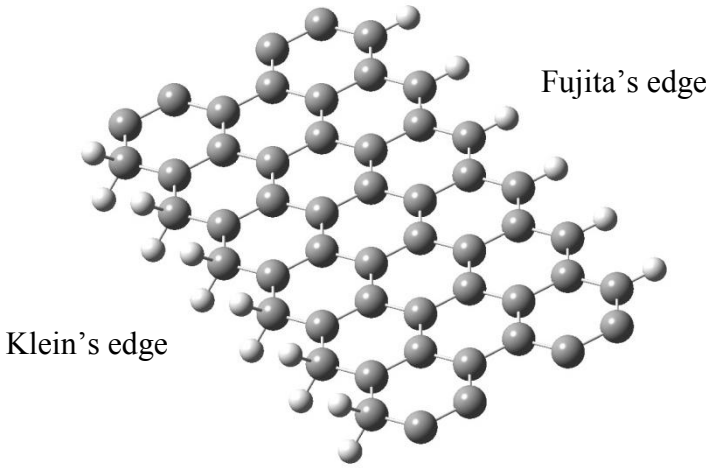

Figure 1.2. Klein and Fujita's edge along the zigzag edges of a graphene fragment.

1.6 Fabrication of Graphene and Graphene Nanoribbons

As pointed out by Geim [4], graphene is not a standard surface nor a standard molecule, so it is receiving little attention from professional chemists. Another probable reason for this scenario lies in the complexities in obtaining this material. Up to now, there has been a few methods to fabricate sheet (or sheets) of graphene. Modifications to these methods are directed to producing graphene that is suitable for large scale industry applications. A few recent review papers that include the fabrication and ways to obtain graphene sheets are available [4,5,118].

Graphene monolayer was first successfully obtained from experiment by using mechanical exfoliation, a process that involves the repeated peeling off of graphite layers from highly-oriented pyrolytic graphite [1]. This method provided a simple way to obtain high quality graphene monolayer, as can be seen from the devices fabricated in this way [2], but it is not viable for industry-scale applications because it is time consuming. Modifications to this method do show some promise in large-scale production. For example, the approach that first bonds bulk graphite to an insulating substrate, and later the graphene layers are cleaved off to leave only single

or few layer graphene on the substrate [119]. Another method is exfoliation in liquid phase [120]. Also, it was shown that exfoliation of graphite oxide upon sonication in water produces graphene sheets [121]. Other methods in obtaining the graphene monolayer are available, such as chemical vapour deposition, chemical methods and thermal decomposition of substrates. A review of the methods used to obtain graphene sheets is given by Choi et al. [118].

As for GNR, the way to produce nanoribbons must include the ability to control the type and the smoothness of edges and the width of the nanoribbons, as the electronic properties of GNR are very much depended on the geometry of the ribbon. A few methods are used to produce GNR. In scanning tunneling microscope lithography, the microscope tip is used to etch the desired pattern of GNRs [89]. It was reported that this method can narrow the width of the GNR down to 10 nm (for armchair-edged GNR). This method provides good stability and reproducibility. For comparison, the smallest width of GNR by electron-beam lithography is ~50nm [61,122]. Another method that can produce GNR is the chemical vapour deposition (CVD) method [88]. Using this method, the smallest width of the GNRs fabricated is ~20 nm. But this method does not really directly produce single GNRs, as the produced GNRs are between 2 to 40 layers. The rough zigzag and armchair edges of GNRs obtained by using this method can be smoothen by using a process known as Joule heating [90]. GNRs can also be synthesized chemically. Li et al. manage to obtained sub-10 nm GNRs by deriving the chemically exfoliated graphite flakes using solution-phase sonication [123]. Analysis on the GNRs obtained this way showed that the GNRs are pristine and are of high quality.

The fabrication of large scale graphene and GNRs are essential for the fabrication of electronic devices at the industry scale. Thus it is of paramount

important to derived ways that can clearly produce the geometries of the graphene and GNRs that one desired, and also meet the industry's requirements. Based on the works stated above, it is clear that there are some promising developments in this area.

1.7 Potential Uses of Graphene

Many devices have been associated with graphene because of the excellent electronic, structural, and mechanical properties it possessed. For example, the value of ~1.0 TPa for single sheet of graphene makes it, up to now, the strongest material [28]. There are also many other desirable properties as mentioned in Section 1.2. The applicability of graphene in nanoelectronic devices show promises in replacing the existing technologies in the near future. With the graphene sheets, carbon-based electronics are presented with innovative devices. This short review is not meant to be an exhaustive review on the devices based on graphene as the inventions based on graphene are progressing very rapidly.

Graphene nanoribbons can function as the building blocks of superconducting transistors [124,125]. The role of graphene in this device is to support the flow of the supercurrent between two superconducting materials. Field effect transistors have also been incorporating graphene, especially those that has a band gap, like GNR [123,126,127] and bilayer graphene [128]. The desired features for using graphene included high current on/off ratio, that is, a parameter to determine how fast a transistor can be switched on and off, and the high current density.

Hydrogen storage is another interesting potential application of graphene sheet. It was reported that calcium atoms which were adsorbed on graphene sheet can act as a medium for hydrogen storage [129,130]. The fact that each adsorbed calcium atom can accommodate 4 to 6 hydrogen molecules makes these kind of systems a high capacity hydrogen storage [129,130]. Another atom that has the same role as calcium on graphene is paladium atom [131]. Adsorption of hydrogen atoms directly onto the surface of graphene is also another possible way of storing hydrogen [132]. The energy barriers of hydrogenation and dehydrogenation in this method show that it is reasonable to predict graphene as a potential medium for hydrogen storage [132]. This prediction is justified as there are reports regarding the full hydrogenation and semihydrogenation on the basal plane of graphene [13-15].

Electromechanical resonators made from graphene sheet are highly sensitive to force and charge. This feature makes it an ideal resonator to act as mass, force, and charge sensors [133]. Another characteristic of graphene sheet also makes it an ideal choice for ultrasensitive sensors. Since graphene is an electronically low-noise material, the change of resistance when a molecule is adsorbed on the basal plane of graphene sheet is detectable. Thus graphene sheet can be used as sensors that are capable of detecting individual gas molecules [134].

Apart from the applications discussed above, graphene has also been predicted to show applicability in other areas. The remarkably high thermal conductivity of graphene sheet (5000 $Wm^{-1}K^{-1}$ for suspended graphene [135] and 600 $Wm^{-1}K^{-1}$ for substrate supported graphene [136] at room temperature) has positioned this material as a candidate in heat conduction and thermal management systems [135,137]. Graphenes can be incorporated into capacitors as electrodes because of the low electrical resistance and a large surface area of graphene, where

with these characteristics, the energy density of the capacitors can be increased [138]. The spin polarizability of the edge state of zigzag-edged GNR is suitable to act as a memory device with the application of a voltage [139]. Graphene sheet can be used as a spin valve structure to act as a medium for spin transport between electrodes [140]. Application of graphene in lasers have also been reported [141], as well as in liquid crystal devices as transparent conductors [142], as current nanoswitches to control current flow [143], and as frequency multipliers for signal generation [144]. Graphene is a remarkable material that has shown high usage versatility. Exploration of the potential uses of graphene has sprung up surprises so far, and it is believed that the surprise will be continued in the future.

1.8 Problem Statements and Scopes of Work

A few topics were studied in this work. The molecular orbitals cluster approach were applied to a few clusters with zigzag-edged and armchair-edged GNRs. The variation of the bond lengths and charge distributions of GNRs as the GNRs are expanded within the same symmetry were examined. Detail analyses were performed on the frontier orbitals, spin densities, charges, and bond lengths as the size of the molecules are systematically increased are also being investigated in order to find the suitable and adequate models that can represent the properties of infinitely long GNR. The results from this part are useful for future investigations. This is of interest since GNRs are positioned as electronics building blocks as they possess band gap [18,60,61]. Also, it is of interest to find the trend of the bond lengths in a graphene sheet, especially at the edge and at the center, because these are the two most possible regions that adsorption of foreign atoms will occurred. The models suggested here, which has certain widths and lengths, can be used as a standard in the

investigation of the electronic and structural properties of GNR-derived systems, for example, adsorption at the edge or the basal plane. With this, it is hoped that the ambiguities when comparing results obtained using clusters of different sizes can be discarded.

As the ground state of electronic configuration of a graphene sheet is not necessarily a closed shell singlet, the actual spin multiplicity of a graphene sheet cannot be overlooked. The right value of a spin multiplicity will determine the correctness of the wavefunction, and it is an important input parameter in a quantum chemistry calculations. But for open shell calculation, a phenomenon known as spin contamination will arise. It is beneficial to get a clearer picture the consequences spin contamination occurs in the electronic calculations of graphene systems.

The final topic studied is to find reference data that can be used in identifying the type of edges of a GNR. A few methods of identification based on optical approaches have been proposed, as summarized in Section 1.4. The study performed here would add an elegant method in this identification. The prediction, based on the results of hyperfine interactions, can be used as a reference to design experiments that use muonium in identifying the graphene edges, without destroying it. This is based on the study of the attachment of muonium on the basal plane of GNRs on two types of edges, zigzag and armchair.

The calculations presented here only involve single-layer graphene, with the hydrogens terminating the dangling bonds at the edges. First principles molecular orbital calculations were employed in this project. This method is adequate in predicting the geometrical and electronic properties of nanostructures, and it is believed that this also applies to graphene nanostructure. The procedures will be available in the subsequent chapter.

1.9 Research Objectives

Based on the problem statements in Section 1.8, the objectives of this research are

1. To study the electronic structure of graphene.
2. To determine the optimum quantum mechanical method (QM) to study the electronic structure of graphene.
3. To obtain appropriate models for graphene nanoribbons (GNR).
4. To study the most probable site of muonium attachment and the possibility of using muonium hyperfine coupling constants in identifying the different types of edges in GNR.

Of all the four objectives listed, objective 2 were discussed in Chapter 3, while objective 3 was reported in Chapter 4. Chapter 5 contains the discussions on objective 4.

REFERENCES

1. K. S. Novoselov, A. K. Geim, S. V. Morozov, D. Jiang, Y. Zhang, S. V. Dubonos, I. V. Grigorieva, and A. A. Firsov, Science **306**, 666 (2004).

2. K. S. Novoselov, D. Jiang, F. Schedin, T. J. Booth, V. V. Khotkevich, S. V. Morozov, and A. K. Geim, Proceedings of the National Academy of Sciences of the United States of America **102**, 10451 (2005).

3. A. K. Geim and K. S. Novoselov, Nature Materials **6**, 183 (2007).

4. A. K. Geim, Science **324**, 1530 (2009).

5. A. H. C. Neto, F. Guinea, N. M. R. Peres, K. S. Novoselov, and A. K. Geim, Reviews of Modern Physics **81**, 109 (2009).

6. T. Ando, NPG Asia Materials **1**, 17 (2009).

7. M. J. Allen, V. C. Tung, and R. B. Kaner, Chemical Reviews **110**, 132 (2009).

8. P. R. Wallace, Physical Review **71**, 622 (1947).

9. S. Mrozowski, Physical Review **92**, 1320 (1953).

10. J. W. McClure, Physical Review **104**, 666 (1956).

11. J. C. Slonczewski and P. R. Weiss, Physical Review **109**, 272 (1958).

12. G. S. Painter and D. E. Ellis, Physical Review B **1**, 4747 (1970).

13. J. O. Sofo, A. S. Chaudhari, and G. D. Barber, Physical Review B **75**, 153401 (2007).

14. D. C. Elias, R. R. Nair, T. M. G. Mohiuddin, S. V. Morozov, P. Blake, M. P. Halsall, A. C. Ferrari, D. W. Boukhvalov, M. I. Katsnelson, A. K. Geim, and K. S. Novoselov, Science **323**, 610 (2009).

15. J. Zhou, Q. Wang, Q. Sun, X. S. Chen, Y. Kawazoe, and P. Jena, Nano Letters **9**, 3867 (2009).

16. P. Sessi, J. R. Guest, M. Bode, and N. P. Guisinger, Nano Letters **9**, 4343 (2009).

17. S. Y. Zhou, G. H. Gweon, A. V. Fedorov, P. N. First, W. A. de Heer, D. H. Lee, F. Guinea, A. H. Castro Neto, and A. Lanzara, Nature Materials **6**, 770 (2007).

18. Y.-W. Son, M. L. Cohen, and S. G. Louie, Physical Review Letters **97**, 216803 (2006).

19. P. Koskinen, S. Malola, and H. Hakkinen, Physical Review Letters **101**, 115502 (2008).

20. T. Wassmann, A. P. Seitsonen, A. M. Saitta, M. Lazzeri, and F. Mauri, Physical Review Letters **101**, 096402 (2008).

21. C. O. Girit, J. C. Meyer, R. Erni, M. D. Rossell, C. Kisielowski, L. Yang, C.-H. Park, M. F. Crommie, M. L. Cohen, S. G. Louie, and A. Zettl, Science **323**, 1705 (2009).

22. B. Huang, M. Liu, N. Su, J. Wu, W. Duan, B.-l. Gu, and F. Liu, Physical Review Letters **102**, 166404 (2009).

23. P. Koskinen, S. Malola, and H. Hakkinen, Physical Review B **80**, 073401 (2009).

24. C. D. Reddy, A. Ramasubramaniam, V. B. Shenoy, and Y.-W. Zhang, Applied Physics Letters **94**, 101904 (2009).

25. J. C. Meyer, A. K. Geim, M. I. Katsnelson, K. S. Novoselov, T. J. Booth, and S. Roth, Nature **446**, 60 (2007).

26. A. Fasolino, J. H. Los, and M. I. Katsnelson, Nature Materials **6**, 858 (2007).

27. J. F. Després, E. Daguerre, and K. Lafdi, Carbon **40**, 460 (2002).

28. C. Lee, X. Wei, J. W. Kysar, and J. Hone, Science **321**, 385 (2008).

29. Z. Ni, H. Bu, M. Zou, H. Yi, K. Bi, and Y. Chen, Physica B: Condensed Matter **405**, 1301 (2010).

30. R. Saito, G. Dresselhaus, and M. S. Dresselhaus, *Physical Properties of Carbon Nanotubes* (Imperial College Press, 2003).

31. T. Morikawa, S. Narita, and T.-i. Shibuya, Journal of Molecular Structure: THEOCHEM **466**, 137 (1999).

32. F. Dietz, N. Tyutyulkov, G. Madjarova, and K. Mullen, Journal of Physical Chemistry B **104**, 1746 (2000).

33. N. Tyutyulkov, K. Müllen, M. Baumgarten, A. Ivanova, and A. Tadjer, Synthetic Metals **139**, 99 (2003).

34. A. Staykov, L. Gehrgel, F. Dietz, and N. Tyutyulkov, Zeitschrift für Naturforschung **58b**, 965 (2003).

35. M. R. Philpott, F. Cimpoesu, and Y. Kawazoe, Chemical Physics **354**, 1 (2008).

36. M. R. Philpott, F. Cimpoesu, and Y. Kawazoe, Materials Transactions **49** 2448 (2008).

37. M. R. Philpott and Y. Kawazoe, Physical Review B **79**, 233303 (2009).

38. M. R. Philpott and Y. Kawazoe, Chemical Physics **358**, 85 (2009).

39. M. R. Philpott and Y. Kawazoe, Journal of Chemical Physics **131**, 214706 (2009).

40. D. Moran, F. Stahl, H. F. Bettinger, H. F. Schaefer, and P. v. R. Schleyer, Journal of the American Chemical Society **125**, 6746 (2003).

41. S. F. J. Cox, S. P. Cottrell, M. Charlton, P. A. Donnelly, C. Ewels, M. Heggie, and B. Hourahine, Journal of Physics: Condensed Matter **13**, 2169 (2001).

42. S. E. Stein and R. L. Brown, Journal of the American Chemical Society **109**, 3721 (1987).

43. N. Tyutyulkov, G. Madjarova, F. Dietz, and K. Mullen, Journal of Physical Chemistry B **102**, 10183 (1998).

44. K. N. Kudin, ACS Nano **2**, 516 (2008).

45. K. S. Novoselov, A. K. Geim, S. V. Morozov, D. Jiang, M. I. Katsnelson, I. V. Grigorieva, S. V. Dubonos, and A. A. Firsov, Nature **438**, 197 (2005).

46. Y. Zhang, Y.-W. Tan, H. L. Stormer, and P. Kim, Nature **438**, 201 (2005).

47. J. van den Brink, Nature Nanotechnology **2**, 199 (2007).

48. P. Neugebauer, M. Orlita, C. Faugeras, A. L. Barra, and M. Potemski, Physical Review Letters **103**, 136403 (2009).

49. K. S. Novoselov, Z. Jiang, Y. Zhang, S. V. Morozov, H. L. Stormer, U. Zeitler, J. C. Maan, G. S. Boebinger, P. Kim, and A. K. Geim, Science, 1137201 (2007).

50. M. Fujita, K. Wakabayashi, K. Nakada, and K. Kusakabe, Journal of the Physical Society of Japan **65**, 1920 (1996).

51. K. Nakada, M. Fujita, G. Dresselhaus, and M. S. Dresselhaus, Physical Review B **54**, 17954 (1996).

52. Y. Miyamoto, K. Nakada, and M. Fujita, Physical Review B **59**, 9858 (1999).

53. Y. Kobayashi, K.-i. Fukui, T. Enoki, and K. Kusakabe, Physical Review B **73**, 125415 (2006).

54. Y. Kobayashi, K. Kusakabe, K.-i. Fukui, and T. Enoki, Physica E: Low-dimensional Systems and Nanostructures **34**, 678 (2006).

55. T. Enoki, Y. Kobayashi, C. Katsuyama, V. Y. Osipov, M. V. Baidakova, K. Takai, K.-i. Fukui, and A. Y. Vul, Diamond and Related Materials **16**, 2029 (2007).

56. J. Y. Wu, J. H. Ho, Y. H. Lai, and M. F. Lin, Physica E: Low-dimensional Systems and Nanostructures **40**, 2019 (2008).